Published in final edited form as:
Mol Cancer Res. 2014 November ; 12(11): 1621–1634. doi:10.1158/1541-7786.MCR-14-0018.

The Anti-proliferative Response of Indole-3-carbinol in human melanoma cells is Triggered by an Interaction with NEDD4-1 and Disruption of Wild-type PTEN Degradation

Ida Aronchik[#], **Aishwarya Kundu**[#], **Jeanne G. Quirit**, and **Gary L. Firestone**
Department of Molecular and Cell Biology and The Cancer Research Laboratory, Univ. of California at Berkeley, Berkeley, CA 94720-3200

[#] These authors contributed equally to this work.

Abstract

Human melanoma cells displaying distinct PTEN genotypes were used to assess the cellular role of this important tumor suppressor protein during the anti-proliferative response induced by the chemopreventative agent indole-3-carbinol (I3C), a natural indolecarbinol compound derived from the breakdown of glucobrassicin produced in cruciferous vegetables such as broccoli and Brussels sprouts. I3C induced a G1-phase cell cycle arrest and apoptosis by stabilization of PTEN in human melanoma cells that express wild-type PTEN, but not in cells with mutant or null PTEN genotypes. Importantly, normal human epidermal melanocytes were unaffected by I3C treatment. In wild-type PTEN-expressing melanoma xenografts, formed in athymic mice, I3C inhibited the *in vivo* tumor growth rate and increased PTEN protein levels in the residual tumors. Mechanistically, I3C disrupted the ubiquitination of PTEN by NEDD4-1 (NEDD4), which prevented the proteasome-mediated degradation of PTEN without altering its transcript levels. RNAi-mediated knockdown of PTEN prevented the I3C induced apoptotic response; whereas, knockdown of NEDD4-1 mimicked the I3C apoptotic response, stabilized PTEN protein levels and down-regulated phosphorylated AKT1 levels. Co-knockdown of PTEN and NEDD4-1 revealed that I3C regulated apoptotic signaling through NEDD4-1 requires the presence of the wild-type PTEN protein. Finally, *in silico* structural modeling in combination with isothermal titration calorimetry analysis demonstrated that I3C directly interacts with purified NEDD4-1 protein.

Implications—This study identifies NEDD4-1 as a new I3C target protein, and that the I3C disruption of NEDD4-1 ubiquitination activity triggers the stabilization of the wild-type PTEN tumor suppressor to induce an anti-proliferative response in melanoma.

Keywords

Indole-3-Carbinol (I3C); anti-proliferative signaling; melanoma cells; PTEN; NEDD4-1

Corresponding Author: Gary L. Firestone, Dept. of Molecular and Cell Biology, 591 LSA, The University of California at Berkeley, Berkeley, CA 94720-3200; Phone: (510) 642-8319; Fax: (510) 643-6791; glfire@berkeley.edu.

The authors have no potential conflicts of interest to disclose.

Introduction

Human melanomas, which arise from melanocytes of neuro-ectodermal origin and can contain mutations in one or more tumor suppressors and/or oncogenes, are the most aggressive form of malignant skin cancers and can be remarkably resistant to conventional cancer therapies (1, 2). Natural dietary phytochemicals represent a promising but largely untapped source of chemotherapeutic agents that has the potential to control the formation, growth and metastasis of human cancers with minimal side effects, especially during prolonged treatments (3–6). Cellular, physiological and epidemiological studies have implicated indole-3-carbinol (I3C), an indolecarbinol compound derived from hydrolysis of glucobrassicin produced in cruciferous vegetables of the *Brassica* genus including cabbage, broccoli and Brussels sprouts, and its natural diindole condensation product 3,3'-diindolylmethane (DIM) as promising anti-cancer phytochemicals with negligible toxicity (5–10). Depending on the human cancer cell type, I3C triggered cell cycle arrest, apoptosis, disruption of cell migration and modulated hormone receptor signaling is mediated by the selective regulation of transcriptional, metabolic, and cell signaling cascades (10–18) (reviewed in 6–9). Many of these anti-proliferative responses are selectively controlled by I3C activated pathways that are unaffected by DIM, which suggests the presence of I3C target proteins that activate specific signaling pathways in different types of cancer cells.

We recently established that I3C and its more potent and stable derivative 1-benzyl-I3C act as direct noncompetitive inhibitors of the proteolytic activity of neutrophil elastase, the first such identified target protein for I3C (19–21). The I3C inhibition of elastase enzymatic activity directly prevents cleavage of the CD40 member of the tumor necrosis factor receptor gene family, which causes CD40 signaling to switch from activating cell survival pathways to triggering anti-proliferative cascades in human breast cancer cells (20, 21). Relatively little is known about the responsiveness of human skin cancers to I3C beyond the observations that I3C increases the sensitivity to UV induced apoptosis and enhances cytotoxic responses in human melanoma (22, 23) and squamous cell carcinomas (24), respectively. Conceivably, the sensitivity of human melanoma cells to I3C may be to due to the expression and function of melanoma expressed indolecarbinol target proteins that can activate anti-proliferative signaling cascades and/or disrupt cell survival pathways.

A variety of genetic alterations in the tumor suppressor PTEN (Phosphatase and Tensin homologue detected on chromosome 10) have been detected in human primary and metastatic melanomas (25, 26). However, many melanomas express very low to nearly undetectable levels of the wild type PTEN due to the loss of heterozygocity, promoter methylation and/or alterations of protein stability (27–30). PTEN dephosphorylates phosphatidylinositol 3,4,5-triphosphate (PIP3) and phosphatidylinositol 3,4-bisphosphate (PIP2) at the cell membrane (31). PIP3 generates membrane-docking sites for both Phosphotidylinositol-Dependent Kinase 1 (PDK1) and for the serine/threonine protein kinase AKT-1 through their pleckstrin homology domains, where PDK1 phosphorylates and activates AKT-1 (31–33). Therefore, low levels of wild type PTEN ensures maintenance of AKT-1-mediated cell survival networks, evasion of apoptosis and enhanced cell invasion properties of human melanoma cells (31–33).

The targeted increase in PTEN level and/or activity in melanoma cells should potentially disrupt the PDK-1 mediated activation of AKT-1 and thereby negatively regulate AKT-1 cell survival signaling (33). Steady state levels of PTEN protein are highly regulated by the E3 ubiquitin ligase NEDD4-1, which specifically targets PTEN for proteasomal degradation (34). In the present study, we demonstrate that I3C selectively stabilizes PTEN protein to induce an apoptotic response in human melanoma cells that express wild type PTEN protein. We further show that I3C disrupts the NEDD4-1-dependent ubiquitination and degradation of PTEN protein, and directly interacts with purified NEDD4-1 protein. Our study implicates this E3 ubiquitin ligase as a biologically significant I3C target protein in human melanoma cells and further suggests that by stabilization of PTEN protein, indolecarbinol-based compounds could potentially be developed in new therapeutic strategies for treatment of human melanoma.

Materials and Methods

Materials

Melanoma cell lines G-361, SK-Mel-28, SK-Mel-30, RPMI-7951, and normal human primary epidermal melanocytes were all purchased from American Type Culture Collection (ATCC) (Manasas, VA), and were authenticated according to the ATCC guidelines. I3C and MG-132 were purchased from Sigma Aldrich (St. Louis, MO). Two different PTEN siRNAs, two distinct NEDD4-1 siRNAs and the corresponding scrambled siRNAs, and the HiPerFect reagents were purchased from Qiagen (Valencia, CA). Antibodies to PTEN, NEDD4-1, ubiquitin, Bcl-2 and MDM-2 were obtained from Santa Cruz Biotechnology (Santa Cruz, CA), the antibody to Hsp90 was purchased from BD Biosciences Franklin (Lakes, NJ) and antibodies to PARP, cleaved PARP, cleaved caspase 3, p53, phosphor-MDM2, Phospho-AKT-1, and AKT-1 were acquired from Cell Signaling Technology (Beverly MA). The secondary anti-mouse and anti-rabbit antibodies conjugated with HRP were obtained from Bio-Rad Laboratories (Hercules, CA). Secondary antibodies conjugated to fluorescent probes were purchased from Molecular Probes/Invitrogen (Eugene, OR). All primers used in RT-PCR reactions were synthesized by IDT technologies (San Diego, CA.)

Cell Culture and Indolecarbinol Treatment

The G-361 melanoma cells were cultured in Modified McCoy's 5A cell media supplemented with 10% fetal bovine serum (Gemini Bio Products, West Sacramento, CA), 2 mM L-glutamine, and 2.5 ml of 10,000 U/ml penicillin/streptomycin mixture (Gibco, Life Technologies, Carlsbad, CA). SK-MEL-28 and SK-MEL-30 cells were cultured in DMEM with 4.5 g/L glucose supplemented with 10% fetal bovine serum, 2 mM L-glutamine, 2.5ml of 10,000 U/ml penicillin/streptomycin mixture in addition to 1X of MEM Non-Essential Amino Acid (Gibco, Life Technologies, Carlsbad CA). RPMI-7951 cells were cultured in DMEM containing 4.5 g/L Glucose, 114 mg/L Sodium Pyruvate, and 2 mM L-glutamine, supplemented as described above. Normal human primary epidermal melanocytes were cultured in Dermal Cell Basal Medium supplemented with Melanocyte Growth Kit (ATCC, Manasas, VA) and 2.5 ml of 10,000 U/ml penicillin/streptomycin mixture. The cells were incubated in tissue culture dishes (Nalgene Nunc, Penfield, NY) at 37°C with controlled humidity and 5% CO2 air content. All treatment conditions used cells at approximately 80%

confluency. I3C was dissolved in 99.9% HPLC grade DMSO (Sigma Aldrich, Milwaukee, WI) and the final dilution was performed in the media aliquots used for treatment. For use of the MG-132 proteasome inhibitor, G-361 and SK-MEL-20 melanoma cells were treated with or without 200 μM I3C for 48 hours, and the cell cultures incubated in presence or absence of 10 μM MG-132 for the last 5 hours of the treatment. The DNA content of propidium iodide stained nuclei from 48 hour I3C treated and untreated cells was determined by flow cytometry as previously described (21).

Western Blot Analysis and Immunoprecipitations

Western Blot analyses of samples electrophoretically fractionated on 8–10% acrylamide gels were carried out as previously described (20, 21). ECL Lightening reagents were used to visualize the primary antibody bound protein bands in nitrocellulose membranes and the results captured on ECL Autoradiography Film (GE Healthcare, Piscataway, NJ). Immunoprecipitations were carried out as previously described (20). The cell lysates were immunoabsorbed using either mouse PTEN-specific antibodies or non-immune antibodies bound to protein-G coupled precleared Sepharose beads. 1% by volume of total protein extracts were separately analyzed as the input control before adding beads and antibodies. Immunoabsorbed and the input material were fractionated in a 12% polyacrylamide gel, transferred to nitrocellulose membranes, and then the samples were probed with ubiquitin- and mouse PTEN-specific antibodies. HSP90 was used as a gel loading control for the input samples. Membranes containing the immunoprecipitated material were stripped and reprobed with a rabbit PTEN-specific antibody as a loading control for total PTEN in the immunoprecipitated samples. Negative control samples containing IgG lacked any immunoprecipitated proteins.

RT-PCR

Total RNA was extracted using the RNeasy extraction kit for mammalian cells (obtained from Qiagen, Hercules, CA) and spectrophotometrically quantified by absorbance at 260 nm. Reverse transcription (RT) reactions were carried out using RT-MMLV reverse transcriptase (Invitrogen, Eugene, OR) and the cDNA was used for PCR reactions using 10 pM of the following primers: PTEN forward CCACCAGCAGCTTCTGCC ATCTCT and reverse, CCAATTCAGGACCCACACGACGG; and GAPDH forward TGAACGGGAAGCTCACTGG and reverse TCCACCACCCTGTTGCTGTA. PCR conditions were as follows: 30s at 94 °C, 30s at 55 °C and 30s at 72 °C for 28 cycles. PCR products were electrophoretically fractionated in 1.5 % agarose gels containing 0.01% Gel Red (Biotium, Hayward, CA) for DNA staining along with 1 kb plus DNA ladder and further visualized by a UV transilluminator.

NucView live cell assay for Caspase 3 activation

Transfected G-361 cells were seeded on 6-well plates at 40% confluency, and after 24 hours incubation the cells were treated with or without I3C for 48 hours. The cells were collected in 1 ml sterile PBS and 1 μl of quenched NucView 488 probe (35) was added to each sample protected from light and incubated on ice for 30 minutes. The fluorescence emitted by the caspase 3 cleaved NucView 488 probe was analyzed using a Coulter Elite flow cytometer (Beckman-Coulter, Brea, CA) and quantified by EPICS software.

SiRNA Transfections

Transfections with siRNA were carried out according to Qiagen HiPerFect transfection protocol as we previously described (19, 20). Briefly, G-361 cells were plated at 50% confluency on 6-well plates in full cell culture media, and 150 ng of siRNA was mixed with 100 µl of media without serum or antibiotics. HiPerFect transfection reagent was then added to the siRNA suspensions. After vortexing, each mixture was incubated for 10 minutes at room temperature, and added to cells in a drop-wise manner while gently agitating to ensure even distribution of the siRNA. The cells were incubated for 24 hours in full growth medium, and after aspirating the medium, the cells were treated in the presence or absence of 200 µM I3C in full growth media for 48 hours, with the media being replaced after 24 hours of treatment.

G-361 cell derived tumor xenografts in athymic mice

Approximately 1 million G-361 cells in a total volume of 0.1 ml of matrigel were injected subcutaneously into each lateral flank of NIH III athymic nude mice. The resulting tumors were allowed to grow to a mean starting volume of 146 ± 10 mm^3. The animals were then randomized into two groups, each containing five mice; a vehicle control group that was treated with DMSO and an I3C treated group that were injected daily in their scruff with 200 mg/kg body weight of I3C. The resulting tumor volumes were measured every alternate day for a period of 19 days using calipers. The tumor volumes were calculated using the standard formula: ($Width^2$ × Length)/2, and changes in tumor volumes were calculated using the formula: 100+{(Tf-Ti)/ Ti X100}, where Tf is the final mean tumor volume and Ti is the initial mean tumor volume. The data represents the means ± S.E.M. (**P< 0.01) for 5 mice / group, each with two tumors, one in each flank. At terminal sacrifice, tumor xenografts were harvested, and a portion of each tumor was fixed in 4% para-formaldehyde for 1 hour at room temperature, followed by a PBS wash and subsequently immersed in 3% sucrose overnight at 4°C. The resulting tissues were embedded in OCT and 10 µm thin sections were taken for immunofluorescence studies using primary antibodies to PTEN, NEDD4-1 and phosphorylated Akt.

Computer-Aided Molecular Binding Simulations

Structures of NEDD4-1 protein domains were obtained from the Protein Data Bank (PDB, http://www.rcsb.org/pdb/home/home.do) with accession numbers 2ONI and 2NSQ for the HECT ubiquitination domain and C2 domain, respectively. The PRODRG server was used to produce the topology files for modeling the I3C structure. NEDD4-1 domain and I3C structures were loaded into the Hex Protein Docking program (http://www.csd.abdn.ac.uk/hex_server/), and binding simulations were performed using shape and electrostatics as restrictive parameters (36). Prior to docking the structures, all water molecules and hetero molecules were manually removed by editing each PDB file. Modeling results were visualized using the PyMol program (37). The schematic diagrams that illustrate the pattern of interactions between the 3-D coordinates of the protein and bound I3C molecule were generated using the LigPlot program (38). Using Hex Protein Docking software, the molecular dynamics and thermo-stability were calculated using free energy simulations. Further validation of the simulation revealed that 97.59% of the amino acids were in the

preferred regions for Phi and Psi angles and zero percent of the amino acids were in disallowed regions. A total of 2000 solutions were analyzed with a grid dimension of 0.6, and the most favorable models were then selected based on E-values. NEDD4-1 amino acid residues that were within 3.5Å from indolecarbinol predicted binding clusters were identified and the alpha-carbon numbers labeled.

Isothermal Titration Calorimetry analysis of I3C interactions with purified NEDD4-1 protein

Isothermal titration calorimetry experiments were performed at 4°C with a reference power of 4 μcal/sec using an ITC200 instrument (MicroCal GE Healthcare Bio-Sciences, Pittsburgh, PA). The purified NEDD4-1 protein and I3C were stored in buffer containing 25 mM Tris-HCl at pH 8.0, 100 nM NaCl, and 2 mM $MgCl_2$. Each titration in the reaction cell used 400 μL of protein at a concentration of 10 μM and 130 μL of I3C up to a concentration of 100 μM. Thirteen 2 μL injections of I3C into the cell containing NEDD4-1 were performed with a duration of 4 sec per injection and 180 sec spacing. To extract the thermodynamic parameters (binding enthalpy and dissociation constant), titration curves were fit by a non-linear, least-squares method. From these data, the changes in enthalpy and free energy were calculated using the following equations: $\Delta G = -RT \ln K$; $\Delta G = \Delta H - T\Delta S$. The binding curve yielded an equilibrium dissociation constant of ~88.1 nM.

Results

Human melanoma cells expressing wild type PTEN are sensitive to the anti-proliferative effects of I3C

To initially determine whether human melanoma cells are sensitive to the anti-proliferative effects of I3C, four human melanoma cell lines, G-361, SK-MEL-30, SK-MEL-28, and RPMI-7951, with distinct mutational profiles (described in Fig 1), as well as human primary epidermal melanocytes, were treated with or without 200 μM I3C for 48 hours and potential cell cycle effects were analyzed by flow cytometry of propidium iodide stained nuclear DNA. This concentration of I3C is optimally effective in other human cancer cell lines (12, 14) as the functional intracellular concentration of this indolecarbinol entering cells is less than 0.3% of the final concentration in the cell culture media (39). As shown in Figure 1, I3C induced a G1 cell cycle arrest of G-361 and SKMEL-30 melanoma cells, both of which express wild type PTEN and wild type p53. In contrast, SK-MEL-28 and RPMI-7951 melanoma cell lines, which display A499G mutant PTEN or null PTEN genotypes, respectively, were relatively unaffected by 48 hour I3C treatment (Fig 1). SKMEL-28 melanoma cells did show some sensitivity to I3C at time points beyond 48 hours (data not shown). Importantly, normal melanocytes were resistant to the I3C (Fig. 1) suggesting this indolecarbinol compound triggers a melanoma-selective response.

I3C down-regulates the ubiquitination and stabilizes wild type PTEN protein levels by preventing its proteasomal degradation

Because the strong I3C anti-proliferative response correlated with the wild type PTEN status of the melanoma cells lines, the potential effects on PTEN expression was assessed in G-361 and SK-MEL-30 cells treated over a concentration range of I3C for 48 hours. Western blot and RT-PCR analysis of PTEN protein and mRNA levels revealed that I3C strongly up-

regulated PTEN protein levels without altering the level of PTEN transcripts in both of wild type PTEN expressing cell lines (Figure 2A). The HSP90 protein and GAPDH transcript gel loading controls remained unchanged throughout the dose response. The maximal I3C response in the G361 cells occurred at somewhat lower concentrations compared to the SK-MEL-30 melanoma cells. Densitometry of the western blots revealed that in G361 cells, treatment with 200 μM I3C stimulated over a 2-fold increase in PTEN protein levels compared to the untreated cells with no increase in PTEN transcript levels (Figure 2B). In SK-MEL-30 cells, the fold stimulation in PTEN protein was much higher, with 200 μM I3C inducing an almost 10-fold increase in PTEN protein levels with no effect on PTEN transcript levels (Figure 2B). In comparison to G361 and SK-MEL-30 cells, I3C had no effect on the levels of the mutant A499G-PTEN expressed in SKMEL-28 melanoma cells, whereas, PTEN expression remained ablated in RPMI-7951 cells, which display a null PTEN genotype (Figure 2C). Normal primary melanocytes express wild type PTEN, however, I3C had no effect on PTEN protein levels (Figure 2C), suggesting a selective effect of I3C in melanoma cells compared to their normal cell counterpart.

To initially determine if I3C up-regulated PTEN protein levels by preventing its ubiquitin-mediated proteasomal degradation, 48 hour I3C treated and untreated cells G-361 and SK-MEL-30 melanoma cells were incubated in the presence or absence of 10 μM MG-132, a 26S-specific proteasome inhibitor, during the last 5 hours of the incubation. PTEN protein was assessed in total cell lysates by western blot analysis. As shown in Figure 2D, in presence of MG-132, PTEN protein levels were observed to increase in cells treated with or without I3C, and the combination of MG-132 and I3C resulted in an enhanced accumulation of PTEN protein. To further determine whether I3C stabilizes PTEN protein through down regulation of its ubiquitination, cells extracts from I3C treated and untreated cells exposed to MG-132 during the last five hours of the incubation were immunoprecipitated with either PTEN-specific or non-immune antibodies and western blots of electrophoretically fractionated samples probed with anti-ubiquitin antibodies. As shown in figure 2E, I3C strongly down-regulated the level of ubiquitinated PTEN under conditions in which the level of immunoprecipitated PTEN protein increased compared to cells not treated with I3C. PTEN-associated ubiquitin was not detected in immunoprecipitations carried out with non-immune antibodies, demonstrating the fidelity of the assay.

I3C induced apoptosis of G-361 melanoma cells requires PTEN

The I3C mediated stabilization of PTEN protein predicts that I3C should disrupt cell survival pathways and potentially induce apoptosis of melanoma cells in a PTEN-dependent manner. One of the key downstream effectors of PTEN is AKT-1, as PTEN dephosphorylates PIP3, and thereby prevents the PDK-1 phosphorylation and activation of AKT-1 at the plasma membrane (31–33). G-361 melanoma cells were treated with a range of I3C concentrations for 48 hours, and the levels of cleaved Poly (ADP-ribose) polymerase (PARP) molecule, which corresponds to apoptosis related DNA repair activity, was compared to the levels of phosphorylated and total AKT-1 protein. As shown in Figure 3A, western blot analysis of total cell extracts using primary antibodies that detect both full-length and cleaved PARP showed that PARP cleavage was maximally induced by treatment with concentrations of I3C that stabilize PTEN and down regulate phosphorylated AKT-1.

The level of total AKT-1 protein and the HSP90 gel loading control remained relatively unchanged under these conditions.

The activity of caspase 3, an upstream regulator of PARP processing, was examined using the highly sensitive NucView488 live cell assay in which the NucView488 probe releases its fluorescent moiety from a quenched state upon specific cleavage by active caspase 3 (35). Treatment of G-361 cells with 200 μM I3C for 48 hours produced a five-fold induction of caspase 3 activity compared to vehicle control DMSO treated cells (Figure 3B). The effect was slightly attenuated by 72 hours, a time point when more cells displayed cytotoxic effects (blebbing, rapid detachment from the plate surface), associated with later stages of apoptosis. To determine the role of I3C induced stabilization of PTEN protein in melanoma cell apoptosis, initially G-361 cells were transfected with either PTEN siRNA or with scrambled siRNA, and caspase 3 activity assessed in cells treated with or without I3C for 48 hours. As shown in Figure 3C, siRNA knockdown of PTEN prevented the I3C induced apoptotic response, whereas, transfected scrambled siRNA had no effect on the indolecarbinol induced apoptosis. Western blots demonstrated the efficiency of the PTEN siRNA knockdown in I3C treated cells compared to the scrambled siRNA controls.

Because of the possibility of off target effects of the PTEN siRNA, siRNA transfections in both G361 and SK-MEL-30 cells were carried out with a different set of PTEN-specific and scrambled siRNAs. As shown in figure 3D, I3C stimulated an increase in PTEN protein in cells transfected with the scrambled siRNA, whereas, transfection with PTEN siRNA efficiently knocked down PTEN protein levels. In both melanoma cell lines, knock down of PTEN disrupted the I3C regulation of phosphorylated Akt and prevented the increase in the apoptotic response based on production of the cleaved caspase 3 (Figure 3D). The production of total Akt-1 was unaffected by either I3C treatment or the PTEN siRNA. Thus, in human melanoma cells expressing wild type PTEN, production of PTEN is required for the I3C apoptotic response.

Direct role of NEDD4-1 in the I3C stimulated accumulation of the PTEN protein and apoptotic response

PTEN protein stability can be regulated by the E3 ubiquitin ligase NEDD4-1, a member of Neural Precursor Cell Expressed, Developmentally Down-Regulated 4 E3 molecules, which attaches ubiquitin moieties to the PTEN protein on residues Lys 289 and Lys 48, effectively targeting it for proteasomal degradation (34). Regardless of the PTEN status, human melanoma cells as well as normal melanocytes express generally similar levels of NEDD4-1 protein in the presence or absence I3C, although the SK-MEL-30 cells did display a reduced level of NEDD4-1 in I3C treated cells (Figure 4A). Because I3C down-regulated PTEN ubiquitination in wild type PTEN expressing melanoma cells, we explored potential connections between I3C and NEDD4-1 that could regulate PTEN protein stability. To initially test the role of NEDD4-1 in the I3C induced stabilization of PTEN protein, NEDD4-1 expression in G-361 cells was knocked down by transfection of NEDD4-1 specific siRNA. A control set of transfections was carried out with scrambled siRNA. Western blot analysis of electrophoretically fractionated cell extracts revealed that siRNA knockdown of NEDD4-1 triggered an accumulation of PTEN protein in I3C treated and

untreated cells similar to that observed after I3C treatment of cells transfected with scrambled siRNA (Fig 4B). Thus, knock down of the NEDD4-1 E3 ubiquitin ligase mimics the effects of I3C on PTEN protein stabilization.

Several downstream effectors of PTEN signaling that are involved in cell survival and/or apoptotic pathways were examined in melanoma cells transfected with either NEDD4-1 siRNA or scrambled siRNA. An increase in PTEN protein would be predicted to reduce the cellular level of phosphorylated AKT-1 (31, 33). As also shown in Figure 4B, siRNA knock down of NEDD4-1 down-regulated the level of phosphorylated AKT-1 in the presence or absence of I3C to a level that closely approximates that observed in I3C treated control cells. Activation of AKT-1 and its other isoforms have been implicated in cell survival pathways in human cancer cells through its phosphorylation of the ubiquitin ligase MDM2 (40), which in turn promotes the MDM2-mediated ubiquitination and degradation of p53, which disrupts the p53 intrinsic apoptotic program (41). Western blot analysis further revealed that G-361 cells transfected with scrambled siRNA, I3C induced the down regulation of Ser 166 phosphorylated MDM2 with a corresponding moderate accumulation of p53 protein. Both effects were mimicked in either I3C treated or untreated cells transfected with NEDD4-1 siRNA (Fig 4B). Consistent with these effects on Ser 166 phosphorylated MDM2, I3C down regulated the level of the Bcl-2 anti-apoptotic proteins (Fig 4B), which is a down stream target of p53 (42) that has been connected to melanoma pathogenesis. Knockdown of NEDD4-1 attenuated Bcl-2 protein levels that was further reduced after I3C treatment (Fig 4B).

To assess the potential effects of NEDD4-1 knock down on melanoma cell apoptosis, G-361 cells were transfected with either scrambled siRNA or NEDD4-1 siRNA, and then incubated with the NucView488 fluorescent probe to assay caspase 3 activity in live cells. Knock down of NEDD4-1 induced a strong apoptotic response in the absence or presence of I3C (Fig 4C, NEDD4-1 siRNA) that was approximately equivalent to the I3C induced caspase 3 activity in control cells transfected with scrambled siRNA (Fig 4C).

As a complementary functional approach, NEDD4-1 production was knocked down in the absence or presence of PTEN knock down by transfection of the corresponding siRNA in both G361 and SK-MEL-30 melanoma cells, and apoptotic signaling in cells examined in comparison those transfected with scrambled siRNA. As shown in Figure 4D, transfection of the PTEN- and NEDD4-1-specific siRNA was highly efficient in knocking down production of the corresponding proteins. In both melanoma cell lines, knockdown of NEDD4-1 stabilized PTEN levels in the presence or absence of I3C, although compared to cells receiving scrambled siRNA, SK-MEL-30 cells transfected with NEDD4-1 siRNA expressed a reduced level of PTEN protein. Also, similar to untransfected SK-MEL-30 cells (Figure 4A), I3C reduced the level of total NEDD4-1 protein in SK-MEL-30 cells transfected with scrambled siRNA (Figure 4D). The I3C stimulated production of cleaved caspase 3 in both melanoma cell lines was completely blocked in PTEN knock down cells, whereas, in NEDD4-1 knock down cells cleaved caspase 3 was produced in I3C treated or untreated cells (Figure 4D). Importantly, co-transfection of siRNA for PTEN along with siRNA for NEDD4-1 in both cell lines resulted in low levels of cleaved caspase 3 in cells

treated with our without I3C (Figure 4D). Thus, I3C regulated apoptotic signaling through NEDD4-1 requires the presence of the wild type PTEN protein.

In silico modeling, secondary structure and isothermal titration calorimetric analyses of I3C interactions with the PTEN-specific ubiquitin ligase NEDD4-1

The essential role of the NEDD4-1 ubiquitin ligase in the I3C induced accumulation of PTEN protein and apoptotic response in human melanoma cells suggests the possibility of a direct functional interaction between I3C and NEDD4-1. Computer-aided molecular binding simulation, which takes into account the known 3-D crystal structure of NEDD4-1 and the chemical structure of I3C, was used to evaluate potential binding sites for I3C within the NEDD4-1 protein structure. A Hex server protein-ligand docking analysis was employed for the initial simulations because of the ability to scan the large NEDD4-1 protein surface for potential docking sites with a small ligand such as I3C (36). *In silico* molecular modeling revealed a potential I3C binding site on the catalytic HECT domain of NEDD4-1, which mediates the ubiquitin ligase activity of the molecule. The electrostatic potential map of the HECT domain shows that I3C binds to a negative surface and forms interactions that are within 4 Å of residues on the HECT domain (Fig 5A). Upon further inspection of the model using the LigPlot program, it is evident that I3C makes Van der Waals interactions (within 3.5 Å) with residues Ser 652, Phe 656, Ile 693, Val 696, Phe 692, Phe 608, Glu 654, Leu 651 (Fig 5B). Calculated force field energy values for the *in silico* defined I3C interaction with the NEDD4-1 HECT domain yielded negative values (E-value = −170.9 KJ/mol), demonstrating that the structures are predicted to be stable. Simulations that used the C2 domain structure of NEDD4-1 displayed no binding interactions with I3C (data not shown), indicating that I3C likely does not interact with this region of the NEDD4-1 molecule.

Isothermal Titration Calorimetry was employed to directly test the thermodynamics and binding of I3C to purified NEDD4-1 protein. Increasing concentrations of I3C were titrated into a solution of NEDD4-1, resulting in an enthalpically favorable exothermic interaction, which is indicative of an I3C interaction with NEDD4-1. To extract the thermodynamic parameters of binding enthalpy and dissociation constant, titration curves were fit by a non-linear, least-squares method. Analysis of the binding of increasing concentrations of I3C to NEDD4-1 protein revealed that this indolecarbinol protein interacts with NEDD4.1 with a calculated equilibrium dissociation constant of approximately 88.1 ± 13.0 μM (Fig 5B).

Effects of I3C on the growth and the levels of PTEN and NEDD4-1 protein in melanoma cell-derived tumor xenografts

To assess the *in vivo* effects of I3C on melanoma cell growth and regulation of PTEN protein levels, G-361 cell-derived tumor xenografts in NIH III athymic mice were first allowed to grow to an average volume of approximately 150 mm^3, and then the mice were injected subcutaneously with either I3C (200 mg/kg body weight) or with the DMSO vehicle control over an 18-day time course. This dose of injected I3C closely corresponds to the level of I3C administered in clinical trials. In vehicle control treated animals, the G-361 cell tumor xenografts showed robust growth, whereas, I3C strongly suppressed the growth rate of G-361cell-derived tumor xenografts (Fig 6A). The resulting tumors from vehicle control treated animals displayed highly concentrated gross tumor vascularization and were dense,

which is consistent with the rapid growth of cells within the tumor (Fig 6A, micrograph insert). In contrast, the tumor xenografts from I3C treated animals were smaller in size and appeared less vascularized (Fig 6A, micrograph insert). Immunofluorescence analysis of 10 μm cryostat sections from tumors excised from I3C treated and untreated animals revealed a strong increase in PTEN protein staining in selective regions of the tumor xenografts from I3C treated animals compared to tumors from vehicle control treated animals (Fig 6B, left set of panels). The areas in the tumors with the most prominent PTEN protein staining were proximal to structures that resembled blood vessels (Fig 6B, right panels). Analyses of the merged images show that in I3C treated animals, a significant fraction of the tumor cells express higher levels of PTEN protein. In independent sets of tumor xenografts from I3C treated and untreated animals, the PTEN, NEDD4-1 and phosphorylated Akt (Akt-p) protein densities were analyzed. As shown in Figure 6C, *in vivo* treatment with I3C induced an increase in PTEN protein and inhibited the presence of phosphorylated Akt without altering NEDD4-1 protein levels.

Discussion

The therapeutic enhancement of cellular PTEN levels or lipid phosphatase activity represents a potential strategy to effectively target melanoma cells that express the wild form of this tumor suppressor protein (25, 26, 31, 32). Relatively little was known about the mechanism by which indolecarbinol compounds mediate their anti-proliferative effects in human melanoma cells. We functionally established that I3C triggers an apoptotic response in human melanoma cells by increasing the level of wild type PTEN protein resulting from its stabilization due to the disruption of the NEDD4-1-dependent ubiquitination and 26S proteasomal degradation of PTEN protein. For example, siRNA knockdown of PTEN prevented and knockdown of NEDD4-1 mimicked the I3C stimulation of caspase 3 activity and apoptotic response, and this NEDD4-1 apoptotic response required the presence of wild type PTEN. Furthermore, we observed that I3C directly interacts with purified NEDD4-1 protein, which identifies this E3 ubiquitin ligase as a new biologically significant I3C target protein that is critical for the control of AKT-1 mediated cell survival cascades in human melanoma cells.

We propose a direct functional connection between I3C apoptotic signaling and the disruption of NEDD4-1 E3 ubiquitin ligase targeting of PTEN protein due to the loss of NEDD4-1 activity and/or protein-protein interactions. *In silico* molecular modeling revealed a potential I3C binding site in the catalytic HECT domain of NEDD4-1, which is responsible for the ubiquitin ligase activity of the molecule. Consistent with the computer simulations, isothermal titration calorimetry directly demonstrated that I3C binds to purified NEDD4-1 protein with a dissociation constant of approximately 88 μM. The C2 and HECT domains of NEDD4-1, which mediate the membrane localization and ubiquitin ligase activity respectively, bind to each other resulting in auto-inhibition of NEDD4-1 activity (43). Conceivably, I3C binding to the HECT domain could potentially inhibit NEDD4-1 activity by stabilizing the C2-HECT autoinhibitory intramolecular interactions. Furthermore, NEDD4-1 activity can be stimulated by specific activators such as the NEDD Family Interacting Proteins, NDFIP1 and NDFIP2, which function by binding to the WW domains of NEDD4-1 via their PY motifs, and thereby abolish the autoinhibitory interactions

between the C2 and HECT domains of NEDD4-1 (43, 44). A recent study showed that a p34 protein interacts with the WW1 domain NEDD4-1 to regulate NEDD4-1 stability and thereby PTEN ubiquitination (45). Consistent with study, in SK-MEL-30 cells, but not the G361 cells, we observed that I3C treatment causes a moderate down regulation of NEDD4-1 protein. Hence, it is conceivable that I3C interactions with NEDD4-1 may potentially alter or disrupt protein binding to NEDD4-1 in a way that down regulates NEDD4-1 activity and/or protein levels and thereby stabilizes PTEN protein. In contrast, one study suggests that NEDD4-1 activity is dispensable for the regulation of PTEN stability and localization in mouse cells and tissue (46), although melanoma or other skin-derived transformed cells were not tested. Conceivably, different regulatory pathways could be acting on PTEN depending on the transformation state or tissue origin of the cells. Studies are currently underway to determine the precise I3C interaction site in NEDD4-1 and to access the functional consequences of the interaction.

The *in silico* predicted I3C interaction site on NEDD4-1 possesses striking structural and chemical similarities with the I3C binding pocket that we characterized in neutrophil elastase, the first identified indolecarbinol target protein (21). Anti-proliferative responsiveness of I3C in human breast cancer cells is mediated by the ability of I3C to act as a non-competitive inhibitor of elastase enzymatic activity (19–21). In contrast to breast cancer cells, anti-proliferative signaling by I3C in melanoma cells is not mediated by the disruption of elastase cleavage of CD40 (data not shown), which implicates NEDD4-1 as a critical I3C target protein in melanoma cells expression wild type PTEN. Thus, an emerging concept from our previous and current studies is that I3C anti-proliferative responsiveness can be triggered in different cancer cell types by the differential expression of distinct I3C target proteins.

Disruption of *PTEN* causing PI3Kinase/AKT activation and *NRAS/BRAF* mutations leading to constitutive activation of signaling via the MAPK pathway are considered two of the key drivers of melanomagenesis (1, 2, 47). Therefore targeting components of these pathways with either single agents or combinations have been a developing therapeutic strategy in recent years. The *BRAF* mutant melanomas showed high dependency on B-RAF kinase activity and so inhibition of the oncogenic B-RAF resulted in striking reduction in tumor volume in preclinical and clinical trials (48). Based on these observations, the FDA approved PLX4032/vemurafenib (Plexxicon) and dabrafenib (Glaxosmithkline) to treat metastatic melanoma, which are two selective and potent inhibitors of the oncogenic BRAF(V600E). However this treatment has been associated with inevitable development of rapid or acquired tumor resistance within months of the initial treatment (49). The therapeutic potential of selective inhibitors of BARF(V600E) have also been restricted by their ability to paradoxically stimulate growth in tumors harboring a wild-type *BRAF* (50). Also, it has been recently reported that loss of PTEN could confer intrinsic resistance to BRAF inhibitors in melanoma cells (51), suggesting that importance of taking into account the activities of different cell signaling cascades in the treatment of human melanomas.

Our study suggests I3C-based compounds have the potential to be developed in new therapeutic strategies for treatment of human melanoma either alone or in combination with other therapeutic compounds to target different aberrant signaling pathways. Furthermore,

given the significant degree of intratumoral heterogeneity in melanoma (1, 2), combinational therapies could conceivably be employed to simultaneously target multiple cell subpopulations within the tumor. In this regard, a combination of BRaf and MEK inhibitors (dabrafenib/trametinib) is now FDA approved for melanoma patients. Human primary epidermal melanocytes that express wild type PTEN were not responsive to I3C, which indicates that I3C should not adversely impact normal skin cell proliferation. The precise mechanism by which normal melanocytes remain resistant to I3C are not know, and we have observed that in athymic mice, injections of I3C over 3 weeks have no apparent effects on animal weight or behavior. Clinical trials for I3C in women at risk for breast cancer have provided a valuable assessment of clinical safety and tolerated doses of I3C (52, 53). Cytotoxicity results from this clinical trial have shown that patients are capable of receiving as high as 800 mg/kg/day I3C without any adverse side effects, which is a concentration that approximates both the 200 μM I3C used in the cultured melanoma cells and the level of I3C used in the *in vivo* tumor xenograft experiments. Our findings implicate I3C as a potential therapeutic for melanomas that express low levels of wild type PTEN protein in a background of either wild type *BRAF* or *BRAF(V600E)* by disrupting the NEDD4-1 mediated ubiquitination of PTEN and enhancing the total levels of this tumor suppressor protein. The development of structural studies on I3C interactions with its potential molecular target NEDD4-1 may provide valuable insight for the design of highly customized I3C derivatives that would more efficiently stabilize PTEN at lower doses and maximize the potential therapeutic effects.

Acknowledgments

We thank Kathleen A. Durkin for her help with the *in silico* modeling during the early stages of the work. We also thank Kevin Poindexter, Lauren Meyer, Michelle Khouri, and Andrew Gabrielson for their helpful suggestions during the writing of this manuscript.

Financial Support: This study was supported by National Institutes of Health Public Service grant CA102360 awarded from the National Cancer Institute. Ida Aronchik was a postdoctoral trainee supported by a National Research Service Grant (CA-09041) awarded by the NIH.

References

1. Chakraborty R, Wieland CN, Comfere NI. Molecular targeted therapies in metastatic melanoma. Pharmgenomics Pers Med. 2013; 6:49–56. [PubMed: 23843700]
2. Banarchi B, Jabbari CA, Vedadi A, Navab R. Molecular biology of normal melanocytes and melanoma cells. J Clin Pathol. 2013; 66:644–48. [PubMed: 23526597]
3. Kawaskaki BT, Hurt EM, Mistree T, Farrar WL. Targeting cancer stem cells with phytochemicals. Mol Interv. 2008; 8:174–84. [PubMed: 18829843]
4. Higdon B, Delage B, Williams DE, Dashwood RH. Cruciferous vegetables and human cancer risk: epidemiologic evidence and mechanistic basis. Pharmacol Res. 2007; 55:224–36. [PubMed: 17317210]
5. Sarkar FH, Li Y. Harnessing the fruits of nature for the development of multi-targeted cancer therapeutics. Cancer Treat Rev. 2009; 35:597–607. [PubMed: 19660870]
6. Ahmad A, Sakr WA, Rahman KM. Novel targets for detection of cancer and their modulation by chemopreventative natural compounds. Front Biosci. 2012; 4:410–25.
7. Aggarwal BB, Ichikawa H. Molecular targets and anticancer potential of indole-3-carbinol and its derivatives. Cell Cycle. 2005; 4:1201–15. [PubMed: 16082211]

8. Ahmad A, Sakr WA, Rahman KM. Anticancer properties of indole compounds: mechanism of apoptosis induction and role in chemotherapy. Curr Drug Targets. 2010; 11:652–66. [PubMed: 20298156]

9. Firestone GL, Sundar SN. Minireview: Modulation of hormone receptor signaling by dietary anticancer indoles. Mol Endocrinol. 2009; 23:1940–7. [PubMed: 19837944]

10. Firestone GL, Bjeldanes LF. Indole-3-Carbinol (I3C) and 3-3'-Diindolylmethane (DIM) Anti-Proliferative Signaling Pathways Control Cell Cycle Gene Transcription in Human Breast Cancer Cells by Regulating Promoter-Sp1 Transcription Factor Interactions. J. Nutrition. 2003; 133:2448S–55S. [PubMed: 12840223]

11. Garcia HH, Brar GA, Nguyen DHH, Bjeldanes LF, Firestone GL. Indole-3-Carbinol (I3C) Inhibits Cyclin Dependent Kinase-2 Function in Human Breast Cancer Cells by Regulating the Size Distribution, Associated Cyclin E Forms and Subcellular Localization of the CDK2 Protein Complex. J. Biological Chemistry. 2005; 280:8756–64.

12. Marconett CN, Sundar SN, Poindexter KM, Stueve TR, Bjeldanes LF, Firestone GL. Indole-3-carbinol triggers AhR-dependent ERalpha protein degradation in breast cancer cells disrupting an ERalpha-GATA3 transcriptional cross-regulatory loop. Molec Biol Cell. 2010; 21:1166–77. [PubMed: 20130088]

13. Marconett CN, Sundar SN, Tseng M, Tin AS, Tran K, Mahuron K, et al. Indole-3-carbinol down-regulation of telomerase gene expression requires the inhibition of estrogen receptor-alpha and Sp1 transcription factor interactions within the hTERT promoter and mediates the G1 cell cycle arrest of human breast cancer cells. Carcinogenesis. 2011; 32:1315–23. [PubMed: 21693539]

14. Brew CT, Aronchik I, Kosco K, McCammon J, Bjeldanes LF, Firestone GL. Indole-3-carbinol inhibits MDA-MB-231 breast cancer cell motility and induces stress fibers and focal adhesion formation by activation of Rho kinase activity. Int J Cancer. 2009; 124:2294–302. [PubMed: 19173291]

15. Jeong YM, Li H, Kim SY, Yun HY, Baek KJ, Kwon NS, Myung SC, Kim DS. Indole-3-carbinol inhibits prostate cancer cell migration via degradation of beta-catenin. Oncol Res. 2011; 19:237–43. [PubMed: 21542459]

16. Sarkar FH, Li Y, Wang Z, Kong D. Cellular signaling pertubations by natural products. Cell Signal. 2009; 21:1541–7. [PubMed: 19298854]

17. Xu Y, Zhang J, Dong WG. Indole-3-carbinol (I3C)-induced apoptosis in nasopharyngeal cancer cells through Fas/FasL and MAPK pathway. Med Oncol. 2011; 28:1343–8. [PubMed: 20628834]

18. Bai LY, Weng JR, Chiu CF, Wu CY, Yeh SP, Sargeant AM, Lin PH, Liao YM. OSU-19, an indole-3-carbinol derivative, induces cytotoxicity in acute myeloid leukemia through reactive oxygen species-mediated apoptosis. Biochem Pharmacol. 2013; 86:1430–40. [PubMed: 24041743]

19. Nguyen HH, Aronchik I, Brar GA, Nguyen DH, Bjeldanes LF, Firestone GF. The dietary phytochemical indole-3-carbinol is a natural elastase enzymatic inhibitor that disrupts cyclin E protein processing. Proc Natl Acad Sci USA. 2008; 105:19750–5. [PubMed: 19064917]

20. Aronchik I, Bjeldanes LF, Firestone GL. Direct Inhibition of Elastase Activity by Indole-3-Carbinol Triggers a CD40-TRAF Regulatory Cascade That Disrupts NFκB Transcriptional Activity in Human Breast Cancer Cells. Cancer Res. 2010; 70:4961–71. [PubMed: 20530686]

21. Aronchik I, Chen T, Durkin KA, Horwitz MS, Preobrazhenskaya MN, et al. Target protein interactions of indole-3-carbinol and the highly potent derivative 1-benzyl-I3C with the C-terminal domain of human elastase uncouples cell cycle arrest from apoptotic signaling. Molecular Carcin. 2012; 51:881–94.

22. Kim SY, Kima DS, Jeong YM, Moon SI, Kwon SB, Park KC. Indole-3-carbinol and ultraviolet B induce apoptosis of human melanoma cells via down regulation of MITF. Pharmazie. 2011; 66:982–7. [PubMed: 22312706]

23. Kim DS, Jeong YM, Moon SI, Kim SY, Kwon SB, Park ES, et al. Indole-3-carbinol enhances ultraviolet B-induced apoptosis by sensitizing human melanoma cells. Cell Mol Life Sci. 2006; 63:2661–68. [PubMed: 17086378]

24. Dahler AL, Rickwood D, Guminski A, Teakle N, Saunder NA. Indole-3-carbinol induced growth inhibition can be converted to a cytotoxic response in the presence of TPA + Ca2+ in squamous cell carcinoma cell lines. FEBS Letters. 2007; 581:3839–47. [PubMed: 17659285]

25. Aguissa-Toure AH, Li G. Genetic alterations of PTEN in human melanoma. Cell Mol. Life Sci. 2012; 69:1475–91. [PubMed: 22076652]
26. Conde-Perez A, Larue L. PTEN and melanogenesis. Future Oncol. 2012; 8:1109–20. [PubMed: 23030486]
27. Lahtz C, Stranzenbach R, Fiedler E, Helmbold P, Dammann RH. Methylation of PTEN as a prognostic factor in malignant melanoma of the skin. J Invest Dermatol. 2010; 130:620–22. [PubMed: 19798057]
28. Stahl JM, Cheung M, Sharma A, Trivedi NR, Shanmugam S, Robertson GP. Loss of PTEN promotes tumor development in malignant melanoma. Cancer Res. 2003; 63:2881–90. [PubMed: 12782594]
29. Zhou XP, Gimm O, Hampel H, Niemann T, Walker MJ, Eng C. Epigenetic PTEN silencing in malignant melanomas without PTEN mutation. Am J Pathol. 2000; 157:1123–28. [PubMed: 11021816]
30. Herbst RA, Weiss J, Ehnis A, Cavenee WK, Arden KC. Loss of heterozygosity for 10q22-10qter in malignant melanoma progression. Cancer Res. 1994; 54:3111–14. [PubMed: 8205526]
31. Wu H, Goel V, Haluska FG. PTEN signaling pathways in melanoma. Oncogene. 2003; 22:3113–22. [PubMed: 12789288]
32. Ming M, He YY. PTEN: New Insights into Its Regulation and Function in Skin Cancer. The J Invest Dermatol. 2009; 129:2109–12.
33. Robertson GP. Functional and therapeutic significance of Akt deregulation in malignant melanoma. Cancer Metastasis Rev. 2005; 24:273–85. [PubMed: 15986137]
34. Wang X, Trotman LC, Koppie T, Alimonti A, Chen Z, Gao Z, et al. NEDD4-1 is a protooncogenic ubiquitin ligase for PTEN. Cell. 2007; 128:129–39. [PubMed: 17218260]
35. Cen H, Mao F, Aronchik I, Fuentes RJ, Firestone GL. DEVD-NucView488: a novel class of enzyme substrates for real-time detection of caspase-3 activity in live cells. FASEB J. 2008; 22:2243–52. [PubMed: 18263700]
36. Ritchie DW, Ghoorah AW, Mavridis L, Venkatraman V. Fast Protein Structure Alignment using Gaussian Overlap Scoring of Backbone Peptide Fragment Similarity. Bioinformatics. 2012; 28:3274–81. [PubMed: 23093609]
37. DeLano WL. Unraveling hot spots in binding interfaces: progress and challenges. Curr Opin Struct Biol. 2002; 12:14–20. [PubMed: 11839484]
38. Wallace AC, Laskowski RA, Thornton JM. LIGPLOT: a program to generate schematic diagrams of protein-ligand interactions. Protein Eng. 1995; 8:127–34. [PubMed: 7630882]
39. Staub RE, Feng C, Onisko B, Bailey GS, Firestone GL, Bjeldanes LF. Fate of indole-3-carbinol in cultured human breast tumor cells. Chem Res toxicol. 2002; 15:101–9. [PubMed: 11849035]
40. Zhou BP, Liao Y, Xia W, Zou Y, Spohn B, Hung MC. HER-2/neu induces p53 ubiquitination via Akt-mediated MDM2 phosphorylation. Nat Cell Biol. 2001; 3:973–82. [PubMed: 11715018]
41. Ogawara Y, Kishishita S, Obata T, Isazawa Y, Suzuki T, Tanaka K, et al. Akt enhances Mdm2-mediated ubiquitination and degradation of p53. T J Biol Chem. 2002; 277:21843–50.
42. Miyashita T, Harigai M, Hanada M, Reed JC. Identification of a p53-dependent negative response element in the bcl-2 gene. Cancer Res. 1994; 54:3131–35. [PubMed: 8205530]
43. Mund T, Pelham HR. Control of the activity of WW-HECT domain E3 ubiquitin ligases by NDFIP proteins. EMBO Rep. 2009; 10:501–7. [PubMed: 19343052]
44. Mund T, Pelham HR. Regulation of PTEN/Akt and MAP kinase signaling pathways by the ubiquitin ligase activators Ndfip1 and Ndfip2. P Proc Natl Acad Sci USA. 2010; 107:11429–34.
45. Hong SW, Moon JH, Kim JS, Shin JS, Jung KA, et al. P34 is a novel regulator of the oncogenic behavior of NEDD4-1 and PTEN. Cell Death Differ. 2014; 21:146–60. [PubMed: 24141722]
46. Fouladkou F, Landry T, Kawabe H, Neeb A, Lu C, Brose N, et al. The ubiquitin ligase NEDD4-1 is dispensible for the regulation of PTEN stability and localization. Proc Natl Acad Sci USA. 2008; 105:8585–90. [PubMed: 18562292]
47. Hodis E, Watson IR, Kryukov GV, Arold ST, Imielinski M, Theurillat JP, et al. A landscape of driver mutations in melanoma. Cell. 2012; 150:251–63. [PubMed: 22817889]

48. Bollag G, Hirth P, Tsai J, Zhang J, Ibrahim PN, Cho H, et al. Clinical efficacy of a RAF inhibitor needs broad target blockade in *BRAF*-mutant melanoma. Nature. 2010; 467:596–9. [PubMed: 20823850]

49. Chapman PB, Hauschild A, Robert C, Haanen JB, Ascierto P, Larkin J, et al. Improved survival with vemurafenib in melanoma with BRAF V600E mutation. N Engl J Med. 2011; 364:2507–16. [PubMed: 21639808]

50. Hatzivassiliou G, Song K, Yen I, Brandhuber BJ, Anderson DJ, Alvarado R, et al. RAF inhibitors prime wild-type RAF to activate the MAPK pathway and enhance growth. Nature. 2010; 464:431–5. [PubMed: 20130576]

51. Paraiso KH, Xiang Y, Rebecca VW, Abel EV, Chen YA, Munko AC, et al. PTEN loss confers BRAF inhibitor resistance to melanoma cells through the suppression of BIM expression. Cancer Res. 2011; 71:2750–60. [PubMed: 21317224]

52. Reed GA, Peterson KS, Smith HJ, Gray JC, Sullivan DK, Mayo MS, et al. A phase I study of indole-3-carbinol in women: tolerability and effects. Cancer Epidemiol Biomarkers Prev. 2005; 14:1953–60. [PubMed: 16103443]

53. Reed GA, Arneson DW, Putnam WC, Smith HJ, Gray JC, Sullivan DK, et al. Single-dose and multiple-dose administration of indole-3-carbinol to women: pharmacokinetics based on 3,3'-diindolylmethane. Cancer Epidemiol Biomarkers Prev. 2006; 15:2477–81. [PubMed: 17164373]

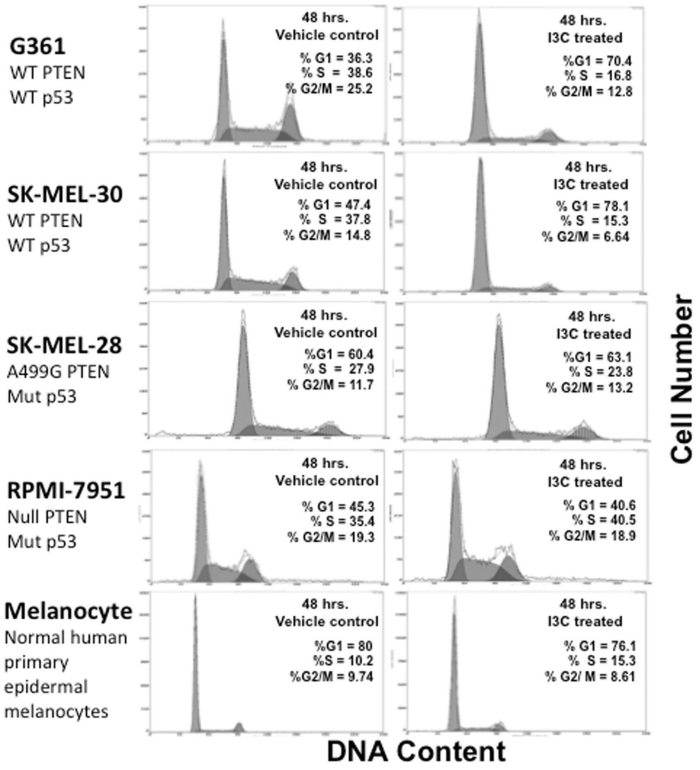

Figure 1.

Cell cycle effects of I3C in human melanoma cells with different genotypes. Cultured human melanoma cell lines that display distinct genotypes (G-361 cells, SK-MEL-30 cells, SK-MEL-28 cells and RPMI-7951 cells) as well as human primary epidermal melanocytes were treated with or without 200 μM I3C for 48 hours. Harvested cells were stained with a hypotonic solution containing propidium iodide, and the DNA content of stained nuclei were quantified by flow cytometry analysis as described in the methods and materials section. The histograms of representative experiments from three independent experiments are shown and the percentage of cells in the population displaying G1, S or G2/M content determined for condition.

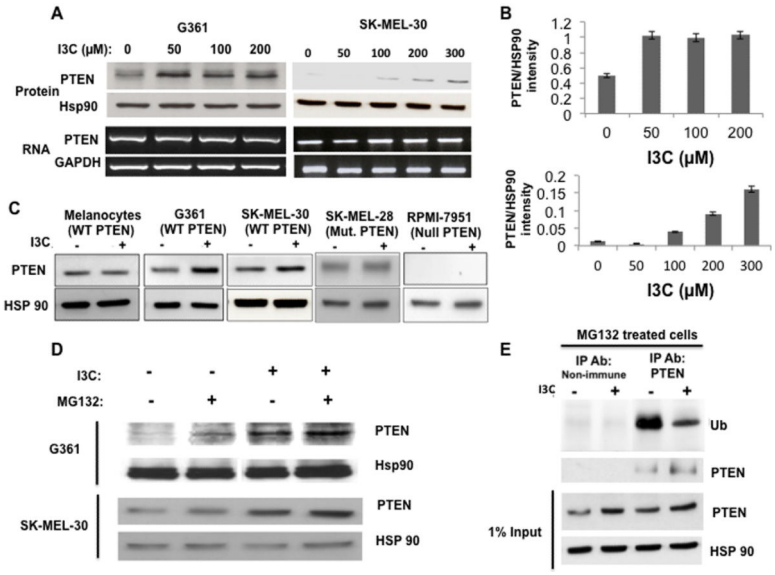

Figure 2.

I3C stimulates the level of wild PTEN protein by down-regulating ubiquitination and preventing the proteasomal degradation of PTEN. (A) G-361 and SK-MEL-30 melanoma cells were treated with the indicated concentrations of I3C for 48 hours. Isolated cell lysates were fractionated by SDS polyacrylamide gel electrophoresis and PTEN protein was monitored by western blot analysis in comparison the HSP90 gel loading control. Representative blots from three independent experiments are shown. Total cellular RNA was isolated, and PTEN transcript expression was determined by RT-PCR in comparison to the GAPDH constitutively expressed control transcript. The PCR products were visualized on a 1% agarose gel stained with ethidium bromide. Representative gels from three independent experiments are shown. (B) At each concentration of I3C, the relative levels of PTEN protein compared to Hsp90 was quantified by densitometry of the western blots shown in Fig 2A. The average protein band intensity from three independent experiments is displayed by bar graphs. (C) Human G-361 and SK-MEL-30 melanoma cells that express wild type PTEN, human RPMI melanoma cells with a null PTEN genotype, human SK-MEL-28 melanoma cells that express an A499G mutated PTEN and human primary epidermal melanocytes that express wild type PTEN were treated with or without 200 μM I3C for 48 hours. Total cell lysates were fractionated by SDS-polyacrylamide electrophoresis and the levels PTEN protein monitored by western blot analysis in comparison the HSP90 gel loading control. Representative blots from three independent experiments are shown. (D) G-361 and SK-MEL-30 melanoma cells were treated with or without I3C for 48 hours and each set of cells were incubated in the presence or absence of 10 μM MG-132, a 26S-specific proteasome inhibitor, for the last 5 hours of the incubation. PTEN protein was assessed in total cell lysates by western blot analysis in comparison to the HSP90 gel loading control. (E) G-361 cells were treated for 48 hours in the presence or absence of I3C, and the cells treated with 10 μM MG-132 for the last 5 hours of the incubation. Cell extracts were immunoprecipitated with either PTEN-specific or non-immune antibodies and western blots of electrophoretically fractionated samples probed with anti-ubiquitin or PTEN-specific antibodies in comparison to the HSP90 gel loading

control. The total level of PTEN protein produced in each condition is shown by the western blot of the 1% input of cell extracts. For clarity of presentation, paired gel lanes of cells not treated with the MG132 26S-proteasome inhibitor were cropped from the upper panel of Fig 2D, which presents the western blot of ubiquitinated PTEN compared to the non-immune antibody control.

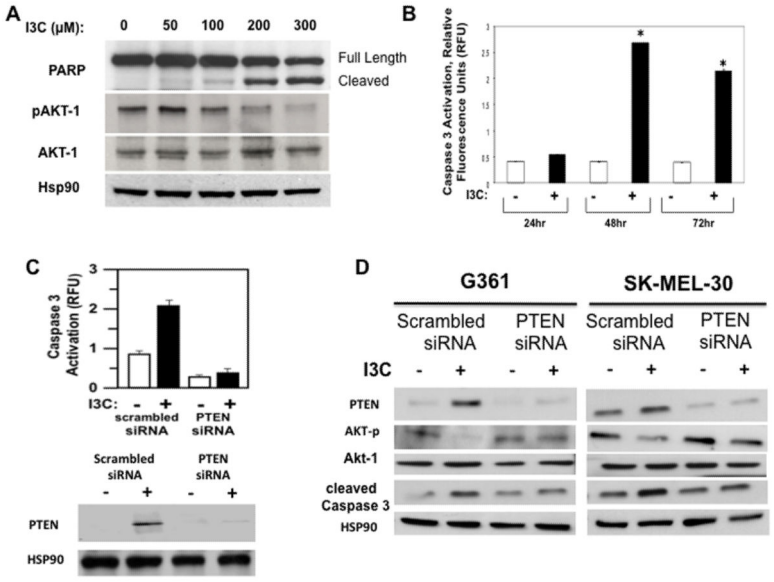

Figure 3.

Role of PTEN in the I3C induced apoptosis of G-361 melanoma cells. (A) G-361 melanoma cells were treated with the indicated concentrations of I3C for 48 hours and protein levels of PARP (full length and cleaved), phosphorylated Akt-1 (pAKT-1), total Akt-1 and the HSP90 gel loading control was determined by western blots of electrophoretically fractionated total cell extracts. (B) G-361 melanoma cells were treated for the indicated times with or without 200 μM I3C and Caspase 3 quantified using the NucView488 live cell assay. Cells treated with NucView488 probe releases a fluorescent moiety from a quenched state upon specific cleavage by active caspase 3. The results are an average of three independent experiments. (C) G-361 cells were transfected with either scrambled siRNA or with PTEN specific siRNA, and then treated with or without 200 μM I3C for 48 hours. Caspase 3 activity was quantified using the NucView488 live cell assay, and the results are an average of three independent experiments. Western blots revealed the level of PTEN protein in cells transfected with each siRNA, and HSP90 was used as a gel loading control. (D) G361 and SK-MEL-30 melanoma cells were transfected with a different set of PTEN and scrambled siRNA and western blots evaluated the levels of PTEN protein, phosphorylated AKT (AKT-p), total Akt-1 and cleaved caspase-3 proteins in comparison to the HSP90 gel loading control.

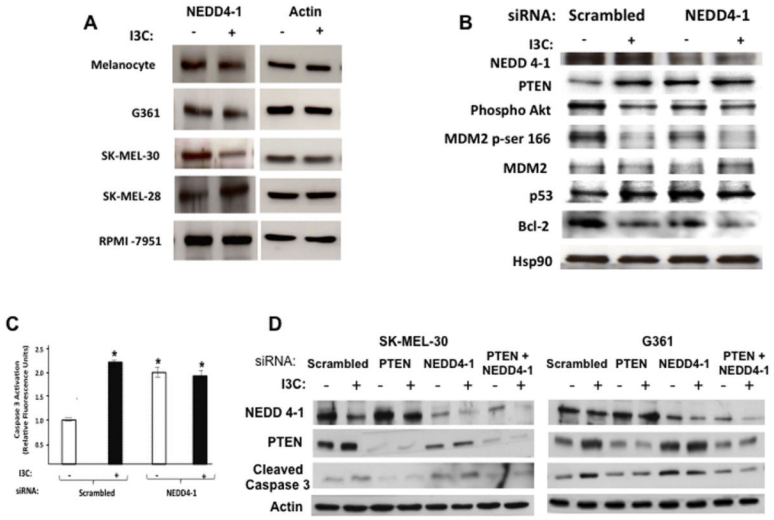

Figure 4.

Role of NEDD4-1 in the I3C induced accumulation of PTEN protein and apoptotic response. (A) Melanoma cells (G361, SK-MEL-30, SK-MEL-28 and RPMI-7951) and melanocytes were treated with or without 200 μM I3C for 48 hours and electrophoretically fractionated cell extracts analyzed by western blots probed for NEDD4-1 protein or actin. (B) G-361 melanoma cells were transfected with either scramble siRNA or with NEDD4-1 specific siRNA and then treated in the presence or absence of 200 μM I3C for 48 hours. Cells were electrophoretically fractionated and western blots probed for production of PTEN, NEDD4-1, phosphorylated Akt-1, Ser-166 phosphorylated MDM2, total MDM2, p53, Bcl-2, and the HSP90 gel loading control. (C) G361 cells were transfected with either NEDD4-1 siRNA or scrambled siRNA, and caspase 3 activity quantified in 48 hr I3C treated and untreated cells using the NucView488 live cell assay. The results are an average of three independent experiments. (D) G361 cells and SK-MEL-30 melanoma cells were transfected with the indicated combinations of NEDD4-1 siRNA and/or PTEN siRNA (different sets of siRNAs from that used in Figure 4B and 4C) as well as with scrambled siRNA and the cells treated with or without 200 μM I3C for 48 hours. Cell extracts were electrophoretically fractionated and western blots probed for NEDD4-1, PTEN, Cleaved PARP and actin.

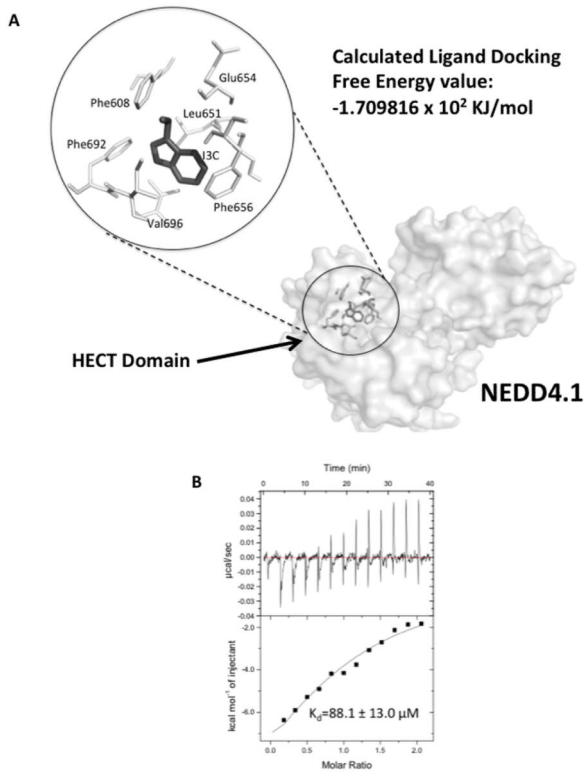

Figure 5.

In silico modeling of predicted I3C interactions with the HECT domain of NEDD4-1 and analysis of I3C binding to NEDD4-1 by Isothermal Titration Calorimetry. (A) Simulations of I3C interactions with HEDD4-1 were analyzed by a Hex server protein-ligand docking program using the 3-D crystal structure of NEDD4-1 and the chemical structure of I3C as described in the methods section. Binding simulations were performed using shape and electrostatics as restrictive parameters, and modeling results were visualized using the PyMol program. The LigPlot program analyzed Van der Waals interactions (within 3.5 Å) between I3C and the NEDD4-1 amino acid residues Ser 652, Phe 656, Ile 693, Val 696, Phe 692, Phe 608, Glu 654, Leu 651. (B) Increasing concentrations of I3C was titrated into a solution of purified NEDD4-1protein and Isothermal Titration Calorimetry quantified the enthalpically favorable exothermic binding interaction. To determine the equilibrium dissociation constant, titration curves were fit by a non-linear, least-squares method.

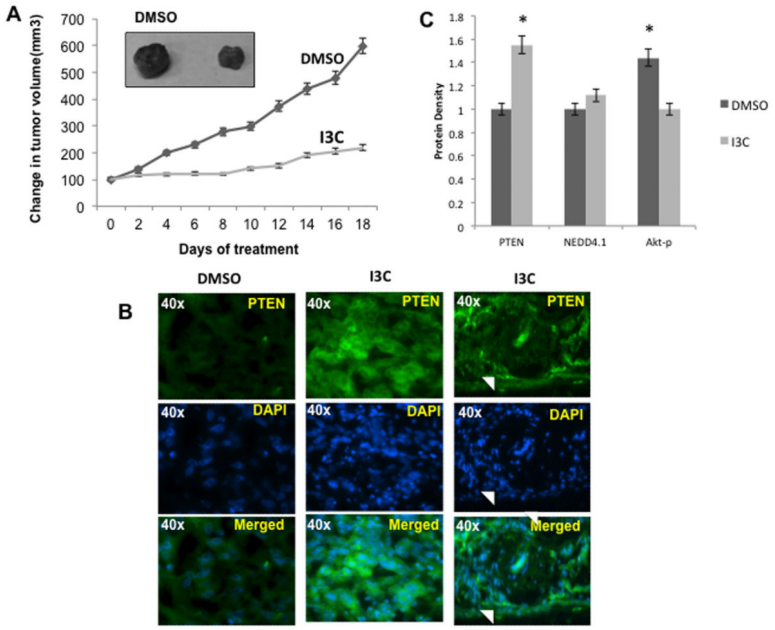

Figure 6.

I3C effects on the growth as well as PTEN, NEDD4-1 and phosphorylated Akt levels in melanoma cell-derived tumor xenografts in athymic mice. (A) One million G-361 melanoma cells were implanted in each lateral flank of NIH III athymic mice, and after palpable tumors were detected (mean starting volume of 146 ± 10 mm^3), the mice were injected subcutaneously with either I3C (200 mg/kg body weight) or with the DMSO vehicle control over an 18-day time course. The resulting tumor volumes were measured and calculated as described in the Methods section. The data represents the means ± S.E.M. (**P< 0.01) for 5 mice / group, each with two tumors, one in each flank. The micrograph insert shows tumors harvested at day 18 from I3C treated or vehicle control treated animals. (B) At terminal sacrifice, the G-361 cell derived tumor xenografts were harvested, and a portion of each tumor was fixed in 4% paraformaldehyde as described in the methods section. 10 μm cryostat sections from tumors excised from I3C treated and untreated animals were analyzed for PTEN expression by immunofluorescence studies using primary antibodies to PTEN. The staining patterns were compared to DAPI staining of the cell nuclei and merged images are shown in the bottom set of panels. (C) The protein densities of PTEN, NEDD4-1 and phosphorylated Akt protein in tumor xenografts from I3C treated and untreated animals were determined by immunofluorescence staining of tumor sections. The results from three independent experiments were quantified.